Supporting information

IR regulation through preferential placement of h-BN nanosheets in a polymer network liquid crystal

Gayathri R. Pisharody,[a,b] Priyabrata Sahoo,[a,b] D. S. Shankar Rao,[a]
H. S. S. Ramakrishna Matte,[a] Debabrata Sikdar,[c] and S. Krishna Prasad[a*]

[a]Centre for Nano and Soft Matter Sciences, Arkavathi, Survey No.7, Shivanapura, Dasanapura Hobli, Bengaluru 562162 (India)
[b]Manipal Academy of Higher Education (MAHE), Manipal, 576104 (India)
[c]Department of Electronics and Electrical Engineering, Indian Institute of Technology Guwahati, Assam, 781039 (India)
skprasad@cens.res.in

Contents

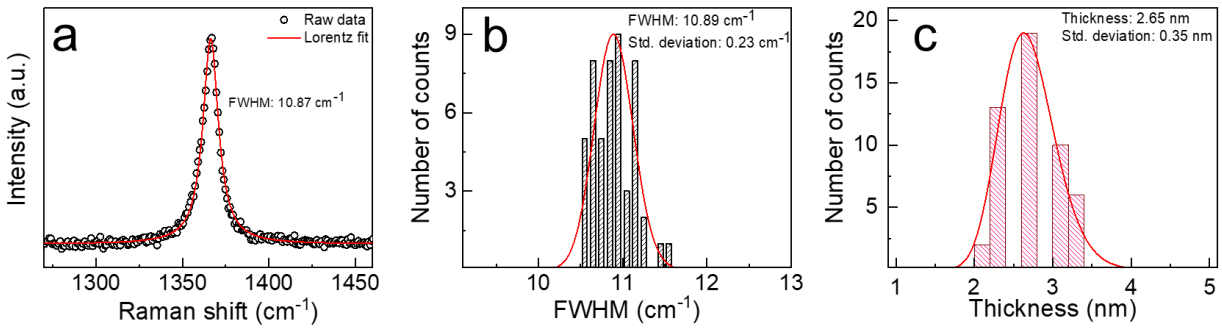

Figure S1: *Determination of layer number and thickness of h-BN nanosheets from Raman spectroscopy. (a) A representative Lorentzian fitting of E_{2g} vibrational Raman mode recorded on h-BN nanosheet, (b) histogram depicting the full width at half maximum (FWHM) derived from fitted Raman spectra, (c) histogram indicating the variation in nanosheet thickness as determined through spectroscopic metrics and considering the monolayer thickness of 0.33 nm.*

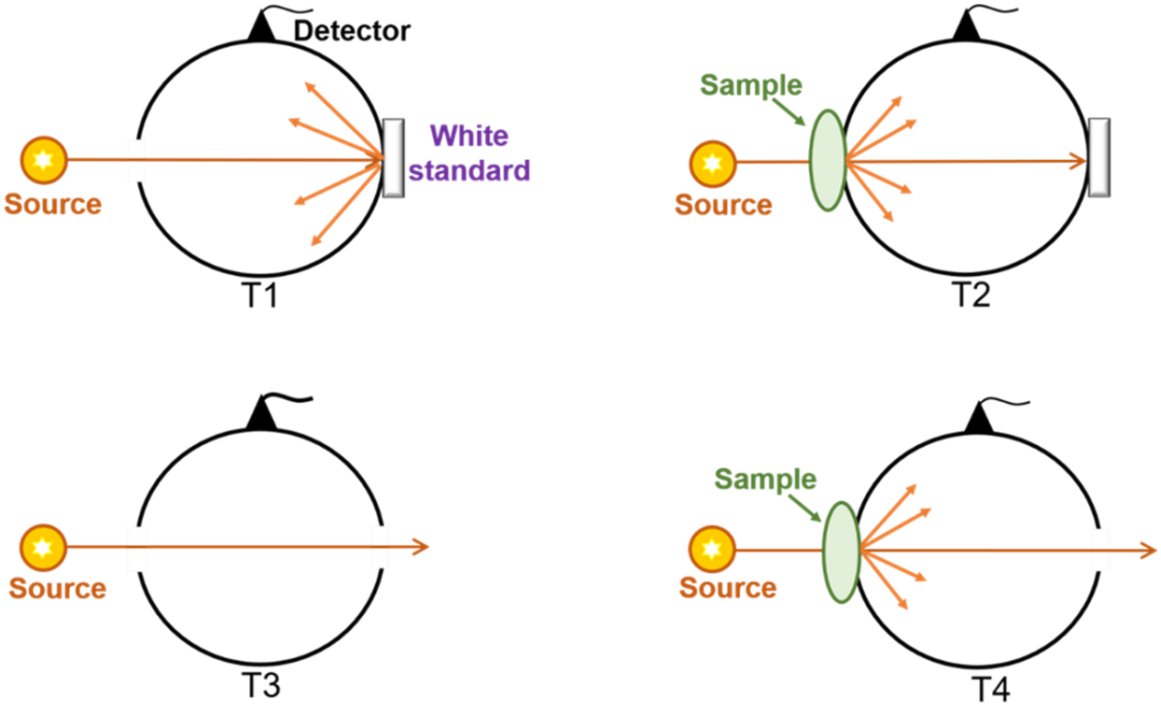

Figure S2: *Schematic diagram representing the measurement of transmittance in four different configurations using which haze is calculated.*

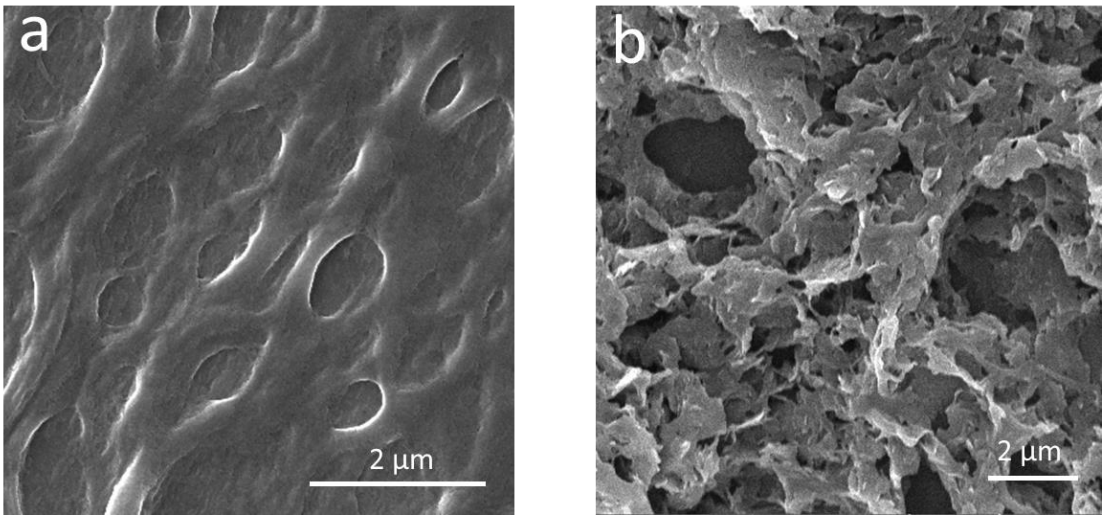

Figure S3*: FESEM image of (a) 3PNLC-0.1BN and (b) 3PNLC-2BN device*

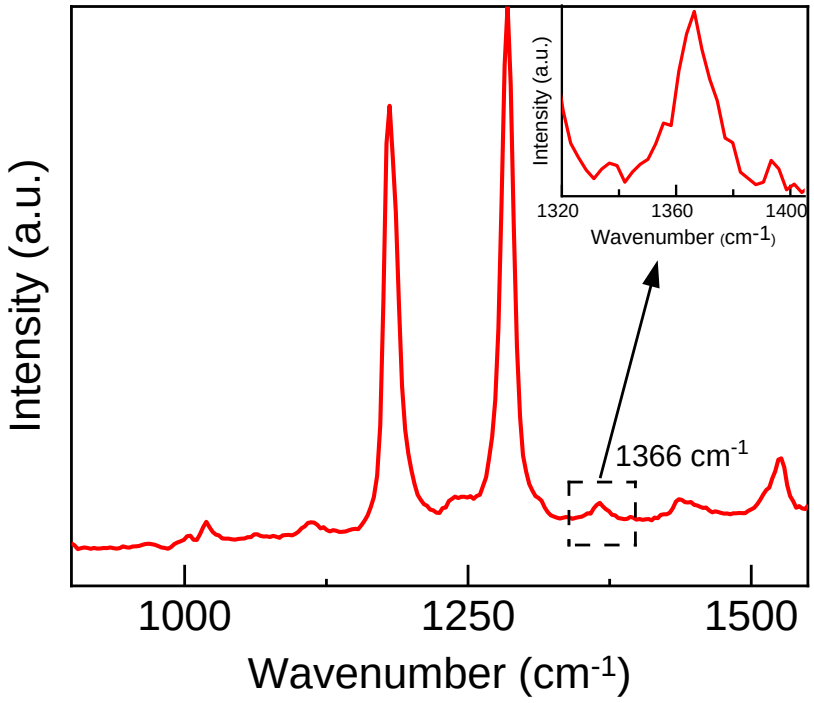

Figure S4: *Raman spectrum of 3PNLC-1BN composite. Inset shows the enlarged image of the fingerprint peak of BN at 1366 cm^{-1}.*

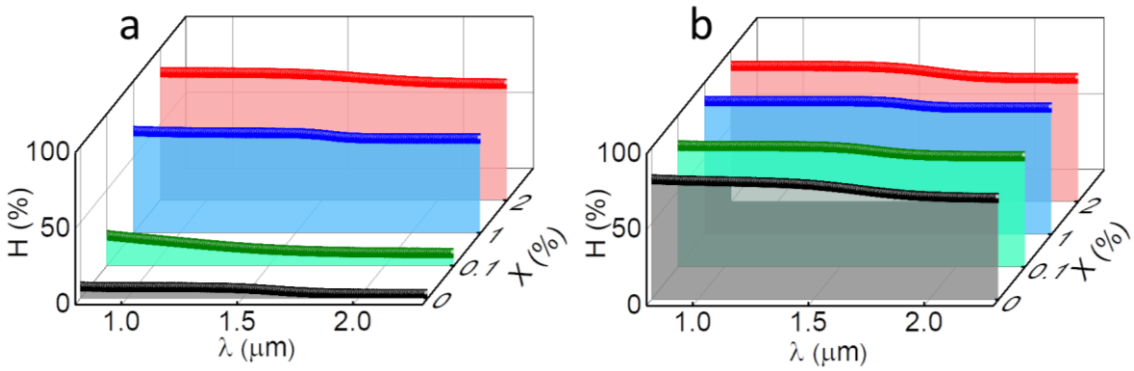

Figure S5: *Haze measurements of 3PNLC (X=0) and 3PNLC-BN at X = 0.1%, 1% and 2% concentrations of BN with the system polymerized in the (a) nematic, and (b) isotropic phase.*

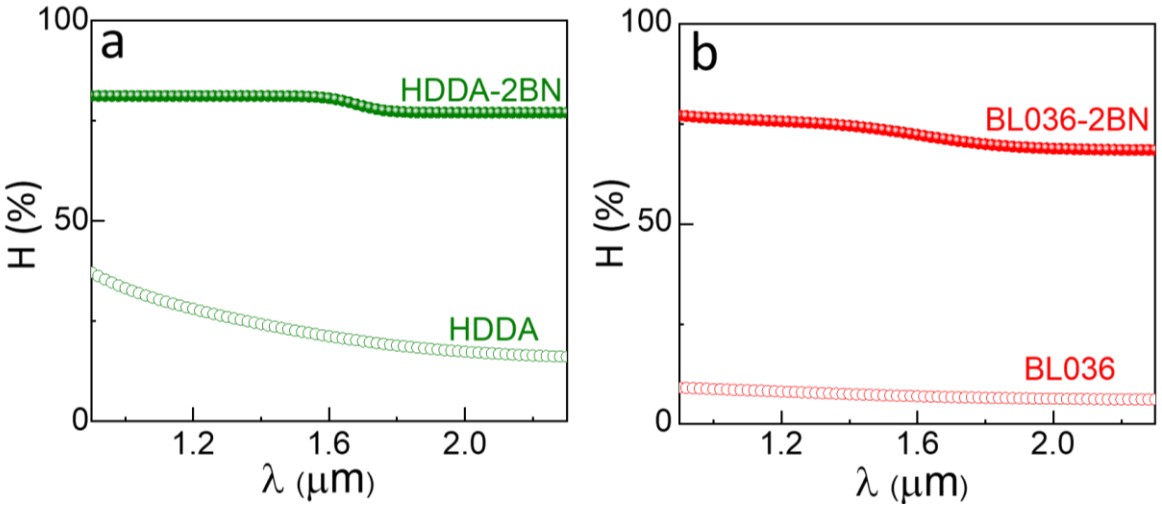

Figure S6: *Comparative haze spectra of four devices, with and without BN inclusions, (a) HDDA and HDDA-2BN whose device compositions are the same as 3PNLC and 3PNLC-2BN respectively, except that the monomer RM82 is replaced with HDDA (b) BL036 and BL036-2BN whose device compositions are same as 3PNLC and 3PNLC-2BN respectively, except that the LC E7 is replaced with another nematic LC, BL036.*

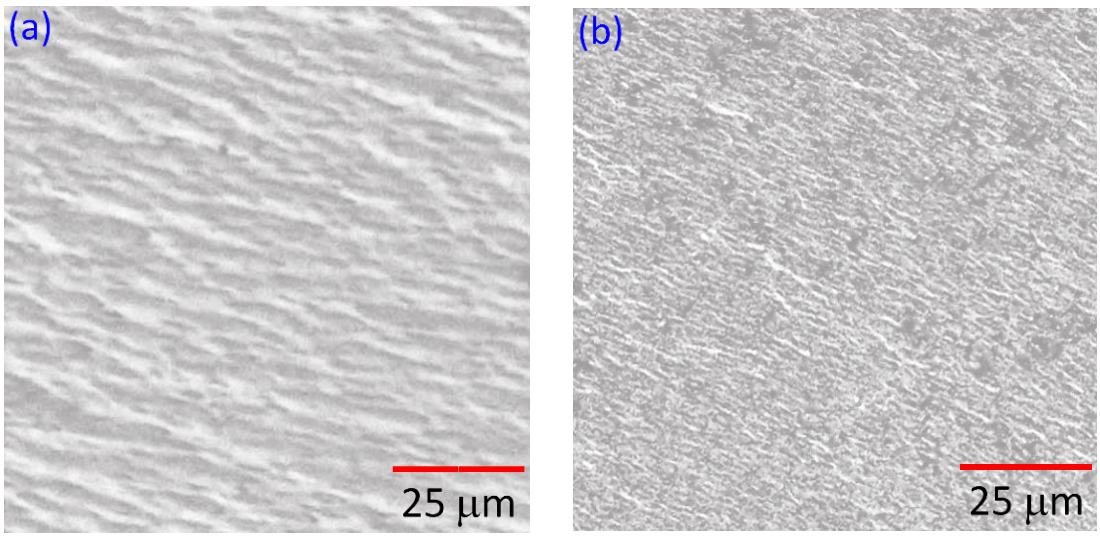

Figure S7*: High-resolution digital microscopy images of (a) PNLC cell with the LC leached out, (b) PNLC cell with the refilled LC+BN mixture leached out (labeled "case 1" in the text). It can be seen that the fibrillar structure is still retained in the latter case.*

.

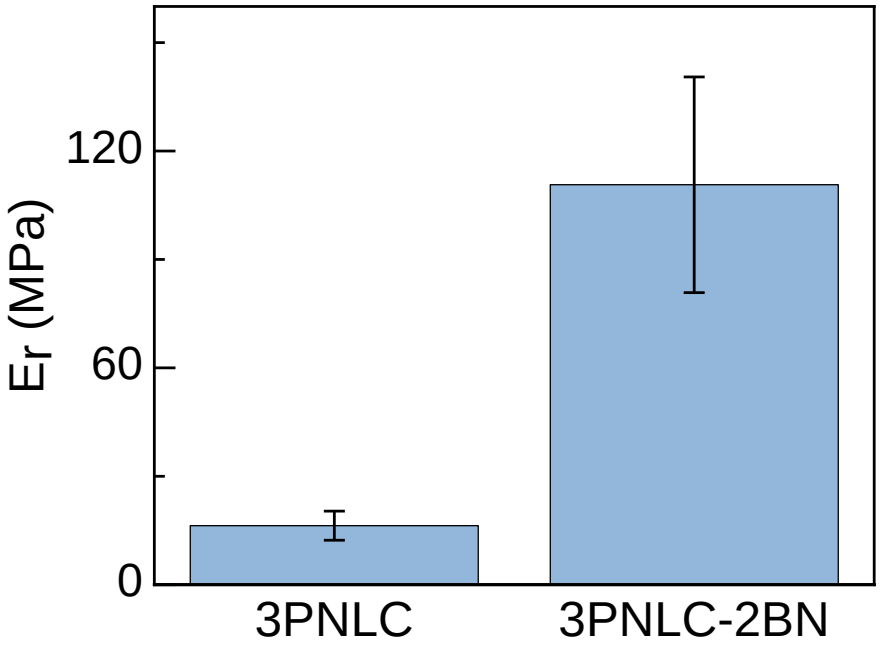

Figure S8: *The reduced Young's modulus (E_r) of the composites 3PNLC and 3PNLC-2BN, measured using a Tribo Indenter system (Hysitron/Bruker, Model TI Premier) with a Berkovich tip. For the measurements under quasi-static loading conditions, indentation tests are performed with a peak load of 100 μN which is maintained for 250s, followed by rapid unloading. Penetration depths (<1μm) of the composites are smaller than 2% of the film thickness, so that the substrate properties are unlikely to influence the measured responses. Reduced elastic modulus is derived by fitting the unloading curve with the power-law relation.*

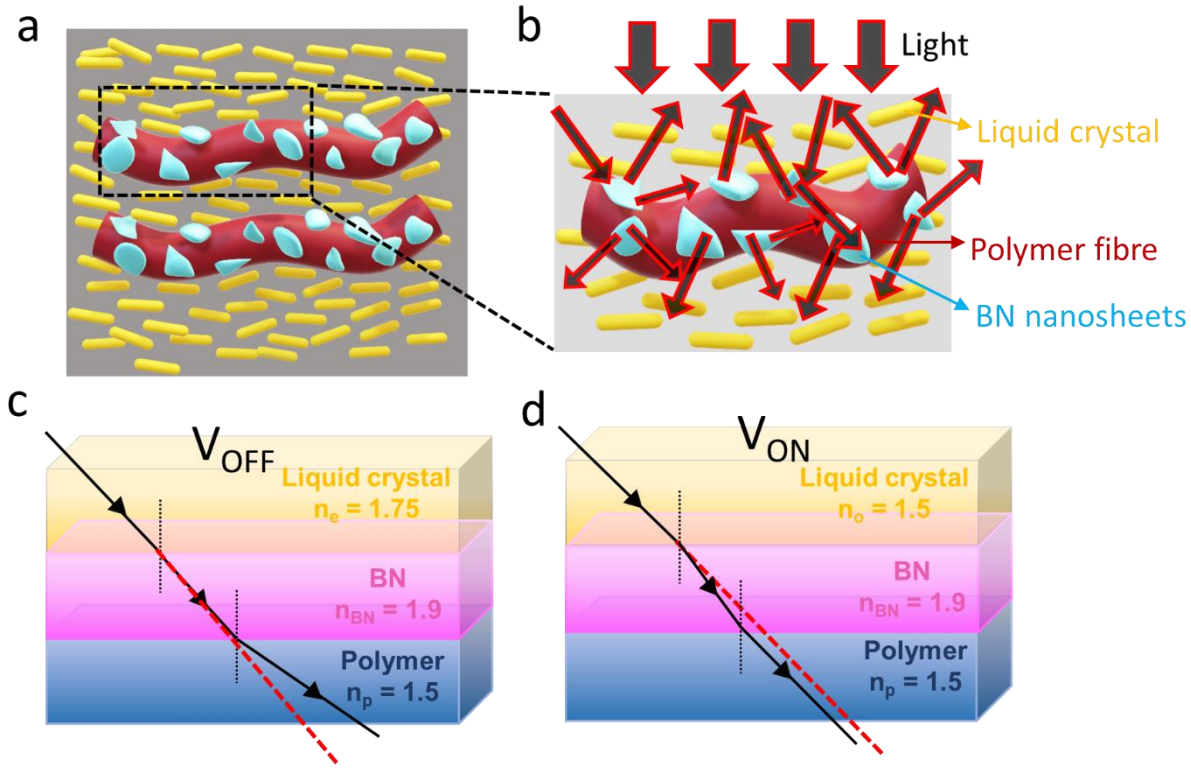

Figure S9: *(a) Schematic showing PNLC-BN architecture, (b) Enlarged image of the schematic (a) showing the enhanced scattering of IR rays by the h-BN nanoflakes. Schematic showing the ray diagram indicating the role of the refractive indices of the different components in controlling the IR scattering under (c) voltage OFF and (d) voltage ON conditions. The red dotted line indicates the extended incident ray.*

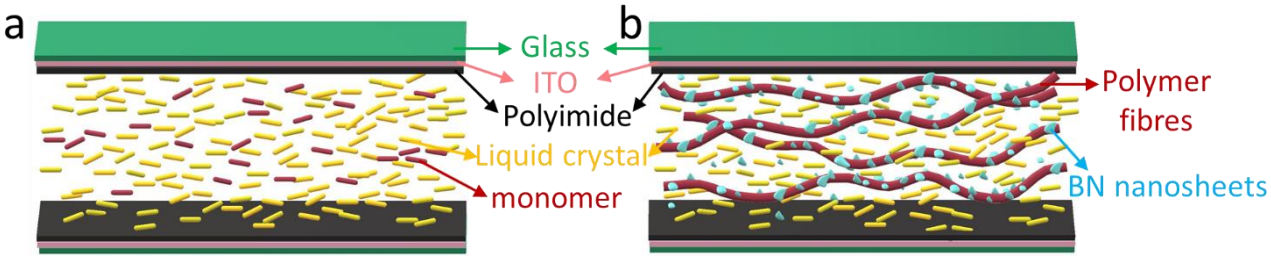

Figure S10: *(a) Schematic of a liquid crystal device (LCD) showing the components: glass (green), indium tin oxide ITO (pink), polyimide alignment layer (black), liquid crystal molecules (yellow) and photo-polymerizable monomers (maroon). (b) Schematic of a PNLC-BN device showing the polymer fibres (maroon) and the h-BN flakes (cyan).*